Investigation of Laminar Flow Around a Blunt and Streamlined Body (Wind Tunnel Laboratory)

Mechanics of Fluids II

School of Mechanical Engineering and Material Science

MEEN40020

Student Name: Ciara Dillon

Student Number: 19370253

Date of Laboratory: 22nd September 2022

Date of Submission: 12th November 2022

Abstract

Aerodynamics and fluid mechanics are vital for the understanding of motion with fluids and bodies and their interactions. This investigation studies the effects of the coefficient of pressure and the effect on the change of angle of attack on the dimensionless parameter. This is very useful for understanding the difference between inviscid and viscous flow, due to the separation of boundary layers in viscous flow and the attached flow for inviscid conditions.

The NACA 0012 symmetrical airfoil was investigated and parameters such as the stall angle and coefficients of drag and lift were analysed with relation to the airfoil's performance. The aerospace industry requires these investigations to maximize performance on airplanes and any streamlined bodies which required minimum drag for higher efficiency.

It was found that he NACA 0012 has an approximate stall angle of 12° in this investigation, found at the maximum value for the coefficient of lift. A software called XFoil was used as a theoretical comparison to the experimental data to allow for evaluation of experimental procedure and assumptions made.

Table of Contents

1. Introduction

The study of fluid mechanics is an area of importance to industries such as aerospace, automobile, medical device. The studies that have been done on the mechanics of fluid flow has been grown from mathematical principles developed by ancient Greek scientists such as Archimedes. These principles, including the basic conservation laws, are the building blocks for why cars have such high efficiencies, why ships travel across oceans, and planes take flight and stay in the sky.

One of the largest reasons for the increased interest in the aerospace industry is throughout the First World War. The 'German Aces' realized that attacking from a higher altitude would allow for them to 'trade potential energy for kinetic energy' and dive for their enemy from above (Bertin and Cummings, 2009). Before WW1, the use of large-scale aircraft as a war tactic was a foreign concept.

Fig 1. WW1 Albatros D. Va 1917 WW1 fighter plane. 1917, flown by the German aces (Grosz, Haddow and Schiemer, 1993)

Through the year 1915, many automobile, and aerospace industries excelled such as Bell and Watsons first transcontinental call. This was the year the National Advisory Committee for Aeronautics (NACA) was created (Bilstein, 1989). In the 1920s NACA technicians designed a wind tunnel at the Langley Laboratory that reached 120 MPH, the best facility in the world, at that time.

Fig 2. Langley Laboratory's first wind tunnel, in the 1920s, (Bilstein, 1989)

From the 1920s to 1930s, the wind tunnel was used to test airfoils designed by NACA, the four-digit number represented the 'critical geometrical properties'. By 1929, a catalogue of 78 airfoils were shown in NACA's annual report, with numbering schemes relating to cross-sectional areas of the airfoils. (Bilstein, 1989).

Airfoils are used for analysis of wings since they are such an important part of the airplane and aerodynamic performance. Different airfoils are used in different parts of airplanes, rotors, blades etc, depending on the function, fluid flow and properties which it is operating against. NACA 0012 is part of the 'four-digit series' of NACA airfoils, the 0012 represents the geometry and indicates that the airfoil has no camber, and the maximum thickness of the airfoil is at 12% of the chord from the leading edge. This airfoil is symmetrical. Its is used for helicopter rudders and rotors as well as flaps in aircraft (Sogukpinar, 2018).

Laminar flow is of high interest currently due to the increased market demand for 'slow flying unmanned aerial vehicles' and 'micro air-vehicles' (MAVs) (Rudmin, Benaissa and Poirel, 2013). Laminar flow over bluff bodies have been investigated for many years to demonstrate the effects of turbulence and geometry of bodies in fluid as shown in Van Dyke's, 'An Album of Motion' in Fig.4.

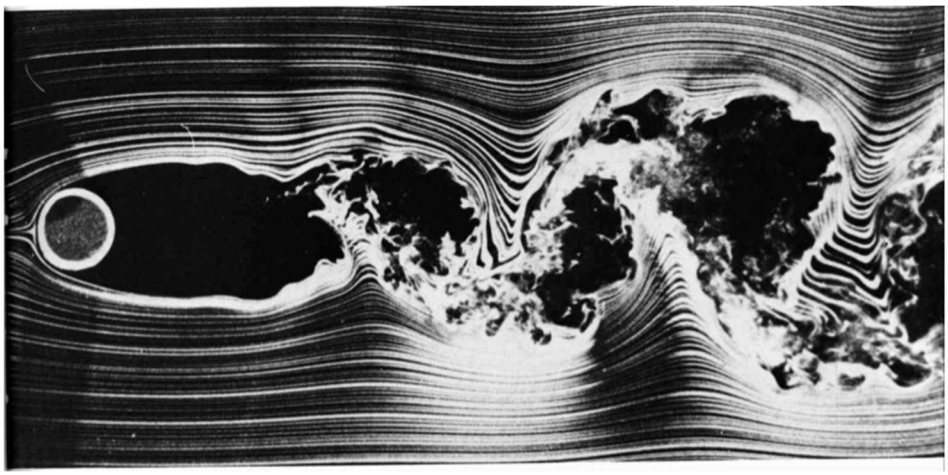

Fig 4 Laminar flow at Re: 10,000 shown over a cylinder (Dyke, 1982)

Fig 4 shows the fluid motion with clear boundary layers, separation of the fluid and turbulence after separation. This image allows the visual understanding of fluid's behaviour at Reynolds's number of 10,000.

2. Objectives

1. Obtain Laminar flow in the wind tunnel to test the flow over bluff and streamlined bodies.
2. To test and analyse the effects of the angle of attack on the coefficient of pressure of a bluff body.
3. To test and analyse the effects of the coefficients of drag and lift of a streamlined body with changing angle of attack.
4. To find the stall angle of the NACA 0012 and the stagnation points of the cylinder in laminar flow conditions.

3. Theory

4.1 Compressibility, Viscosity and Bernoulli's Equation

Compressibility

It takes a large amount of force to increase the density of a fluid, compressible flow requires a very high volume of fluid to be contracted in a smaller section at high speeds. As long as the air velocity in the wind tunnel is below 124.112 m/s it can be assumed the effects of compressibility to be negligible throughout this laboratory. (Anderson, 2007).

Viscid versus Inviscid Flow

For an inviscid fluid flow, the Reynolds number is infinity. Therefore, the viscous effects of the fluid do not affect the boundary layer of the fluid. Creeping flow represents close to inviscid flow. Reynolds number is dependent on the effects of viscosity.

Bernoulli's Equation: Incompressible Flow

$$p_1 + \tfrac{1}{2}\rho V_1^2 = p_2 + \tfrac{1}{2}\rho V_2^2$$

Equation 1. (Anderson, 2007)

From Bernoulli's Equation one can relate the pressure differences in a closed volume from inlet and outlet to their corresponding velocities which is very useful for studying fluid flow properties and concepts of lift and drag.

Derived from momentum equations it is Newton's second law for inviscid incompressible flow without body forces.

For a pitot static probe, from Bernoulli's Equation it can be summarized in the following equation:

$$\underset{\text{static pressure}}{p_1} + \underset{\text{dynamic pressure}}{\tfrac{1}{2}\rho V_1^2} = \underset{\text{total pressure}}{p_0}$$

Equation 2. (Anderson, 2007)

Equation 2 is derived for incompressible flow only. The apparatus and points of measuring pressure and velocity are shown in Fig. 4 for a Pitot Static tube.

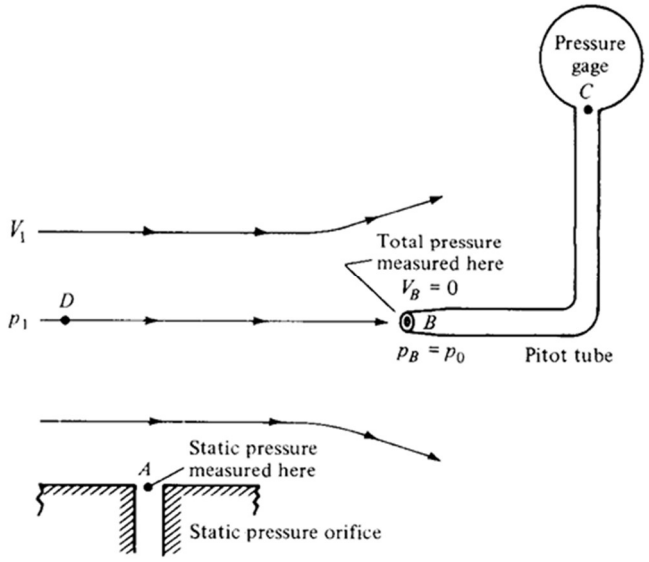

Fig 5. Pitot Tube and Static Pressure Orifice. (Anderson, 2007)

4.2 Open-return Wind Tunnel

The function of a wind tunnel in the study of fluid mechanics is the immersion of an object in an established flow and analysing the disturbance of the object in the flow.

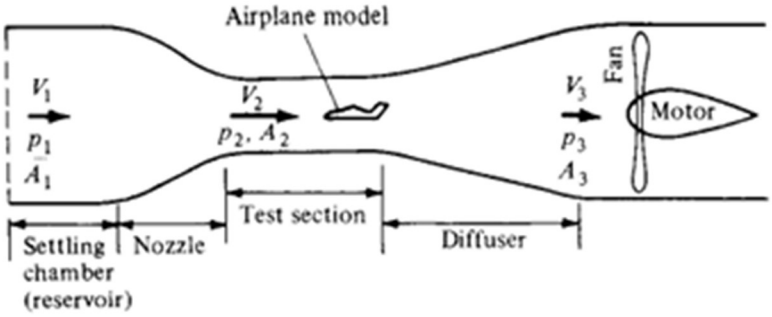

Fig 6. Open-circuit Wind Tunnel (Anderson, 2007)

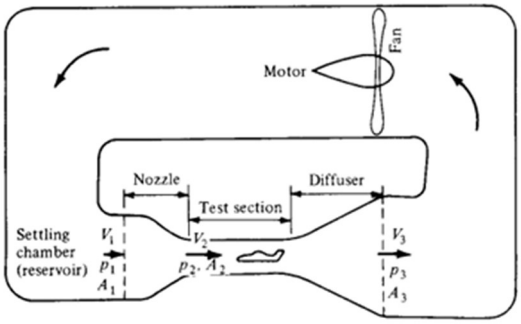

Fig 7. Closed-circuit Wind Tunnel (Anderson, 2007).

The choice between a closed-circuit and open-circuit tunnel is based on the application of the wind tunnel.

4.3 Lift, Drag, Pressure and their coefficients

Aerodynamic forces result from two distributions over a body surface, the pressure distribution and the shear stress (τ) distribution (Anderson, 2007). A total force component (resultant) is analysed on a body and divided based on their direction compared to the body's geometry and surrounding fluid flow. Pressure acts normal to the surface of the body and τ acts in the tangential direction to the surface.

Lift is the upward force on a body perpendicular to the relative motion of the fluid in contact with the body.

The coefficient of lift is the total lift force divided by the kinetic forces on the body's area.

$$C_L = \frac{L}{\frac{1}{2}\rho U^2 S}$$

Equation 1. (O'Rourke, 2022)

Drag is the net force in the direction of the fluid flow around the body due to wall shear stress and pressure (Gerhart, Gerhart and Hochstein, 2017). Pressure drag and friction drag produce net drag forces on the body.

The drag coefficient Eq. 2, a function of other dimensionless parameters such as Reynold's number, is used to compare the drag forced on different geometrical areas of bodies. The Drag coefficient is calculated using Equation 1.: the ratio of total drag on the body divided by the kinetic energy.

$$C_D = \frac{D}{\frac{1}{2}\rho U^2 S}$$

Equation 2. (O'Rourke, 2022)

Estimating the skin friction coefficient using Blasius solution for laminar boundary layers is:

100% Laminar BL:

$$C_{f_{lam}} = \frac{1.328}{\sqrt{R_e}}$$

Equation 3. (Nastase, 2008)

where R_e = Reynolds number.

For an airfoil, the planform area is used to calculate the drag and lift coefficients (Anderson, 2007). Similarly, area S value when analysing the coefficients for the cylinder will use the cross sectional area (Anderson, 2007), due to the orientation of the cylinder in the wind tunnel as show in Fig 8.

The pressure coefficient C_P is a dimensionless parameter is the ratio of pressure difference to dynamic head. C_P is very useful for analysing stagnation points along a body since the stagnation point is when the local velocity over the body is zero. It is noted that C_P does not depend on the geometrical properties of the body or free-stream flow conditions.

$$C_p = \frac{p - p_\infty}{\frac{1}{2}\rho_\infty U_\infty^2} = 1 - \frac{U^2}{U_\infty^2}$$

Equation 4. (Bertin and Cummings, 2009)

For an inviscid flow, the calculation for C_P is using Equation 5.

$C_P = 1-4\sin(\theta)^2$ Equation 5. (Bertin and Cummings, 2009)

4.4 Reynolds Number

Determining if a boundary layer is laminar or turbulent is done by calculating the local Reynold's number on the body. From this calculation the boundary layer thickness as well as the momentum thickness can be determined.

$$\mathrm{Re}_x = \frac{Ux}{\nu}$$ Equation 5.

υ=kinematic viscosity

x = distance from leading edge of the body

U = freestream velocity

4.5 Body Classification

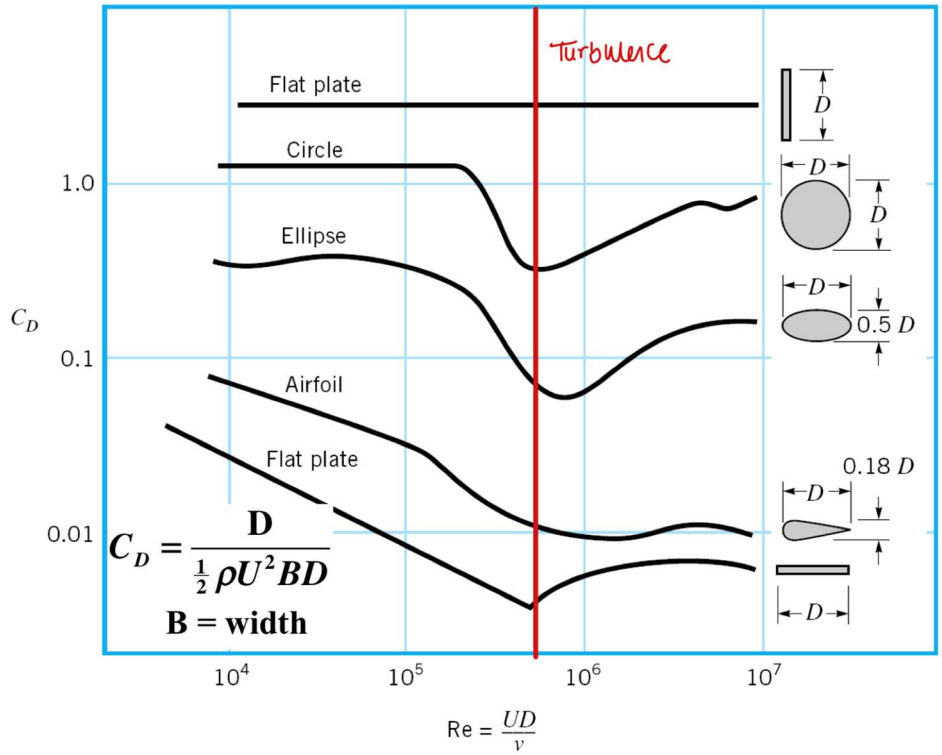

Fig 8. Diagram of Alternative body shapes and the effects of Reynolds's number on the Coefficient of Drag. (K..Nolan, MEEN40020 External Flow Notes)

Bluff Bodies:

A bluff body is a body that has a shape that causes a separated flow over a large part of its surface. The cylinder is a bluff body since "the flow streamlines do not follow the surface of the body"(Straw, 2000) . This separation is due to the cylinder's interaction between the viscous and inviscid regions.

Streamlined Bodies: Airfoils

A streamlined body is one whose shape allows for the streamlines to flow over the bodies surface without separation. The smooth surface prevents turbulence, wakes and vortexes downstream for

lower Reynolds number. The smooth surface reduced friction drags and results in lower losses in the surrounding fluid flow.

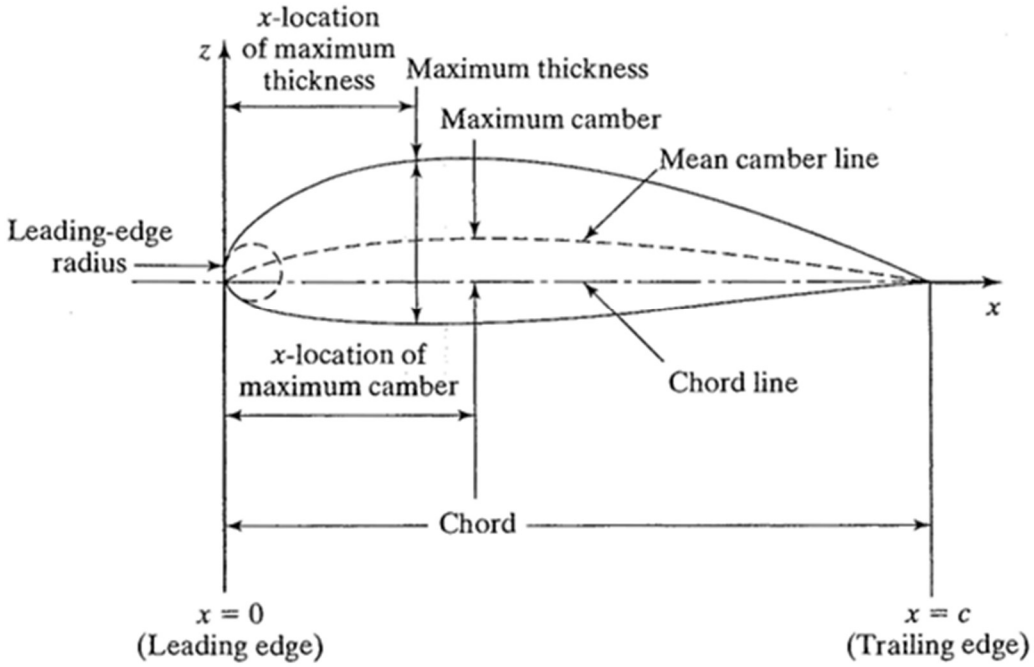

Fig 9. Airfoil-section geometry and nomenclature.(Bertin and Cummings, 2009)

5. Experimental Methods:

5.1 Equipment

Plint Low Speed Wind Tunnel (457 mm x 457 mm)

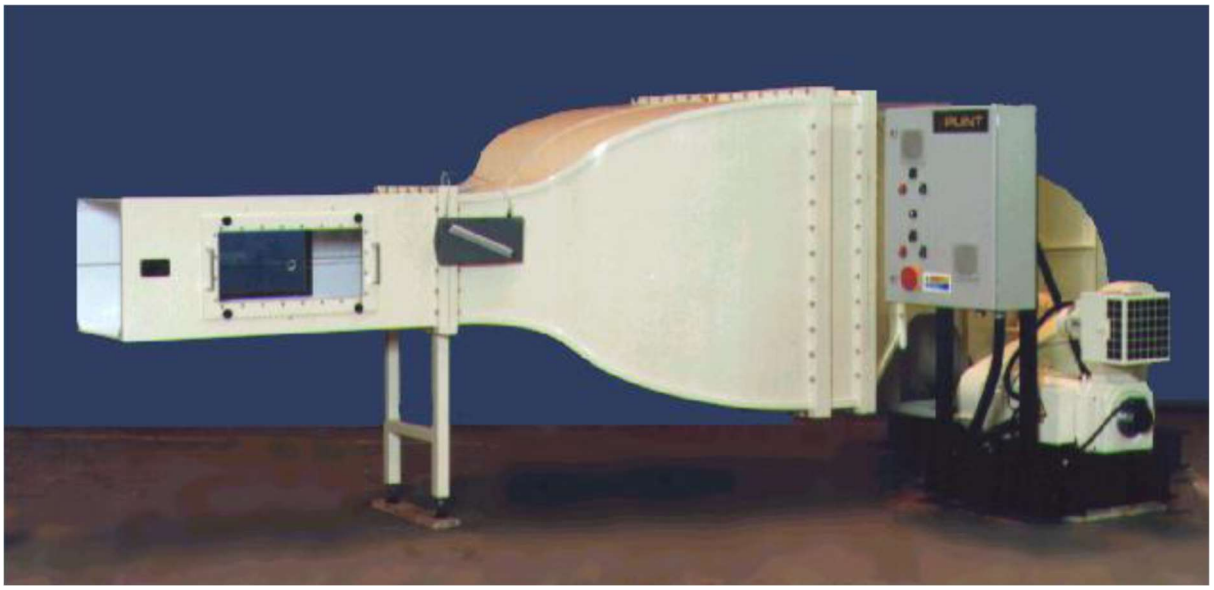

Fig. 10 Low speed wind tunnel (Plint) in Mechanical Engineering Laboratory. (O'Rourke, 2022)

The wind tunnel that was used in this experiment is of closed working section, open return type. The source of air in the tunnel is called a 'thyristor controlled variable speed fan', which delivers air to the short diffuser. A smooth screen and a contraction cone are fitted in the wind tunnel. To allow for laminar flow to be produced and to reduce turbulence entering the testing section of the tunnel a turbulence. The air is diffused out into the atmosphere after flowing through the testing section. The maximum air speed in the working section is 33 m/s (O'Rourke, 2022)

Models:

1. Circular Cylinder (diameter: 76 mm, span length: 455 mm)

Fig 11. Side view of cylinder placed in testing section of low-speed wind tunnel in UCD Mechanical Engineering Lab.

- Airfoil: NACA 0012 (chord length: 152 mm, span length: 455 mm)

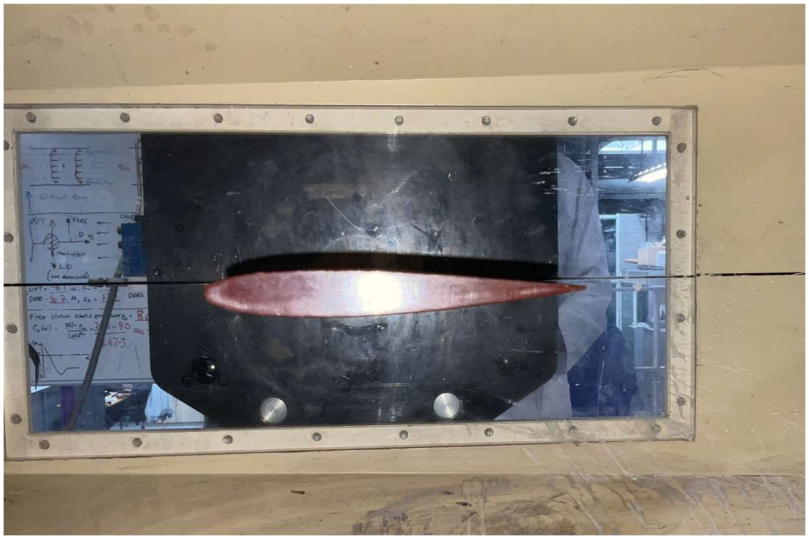

Fig.3 Side view of the NACA 0012 set in testing section - in the wind tunnel laboratory, UCD Mechanical Laboratory

5.2 Instrumentation

Three Component Balance

On the sidewall of the wind tunnel to measure the lift and drag. Essentially a weighing scaled which the model is mounted on, forces are directly measured from the load cells within the balance. It measures the horizontal and vertical forces using a digital meter on the control panel.

Fig 4.a)

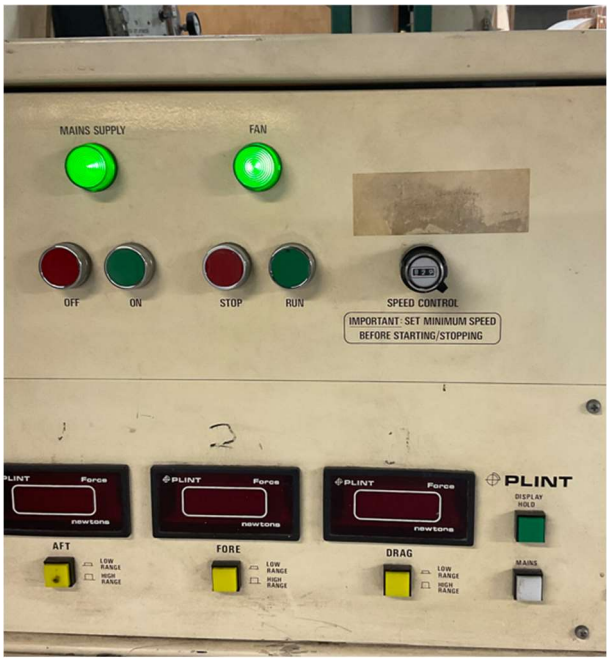

Fig. 4.b)

Fig 4. a) Component Balance mounted vertically on wall of wind tunnel in Mechanical Engineering Laboratory UCD 4.b) Electronic display to show the drag and lift values from the wind tunnel.

Probes

A Prandtl tube and total-static tube are used to measure the dynamic head at the end of the wind tunnel. They are mounted in the traversing mechanism.

Differential Manometer

A differential manometer is used in the laboratory using Prandtl or total-static probes.

Water Manometer – to measure the RPD (reference pressure difference)

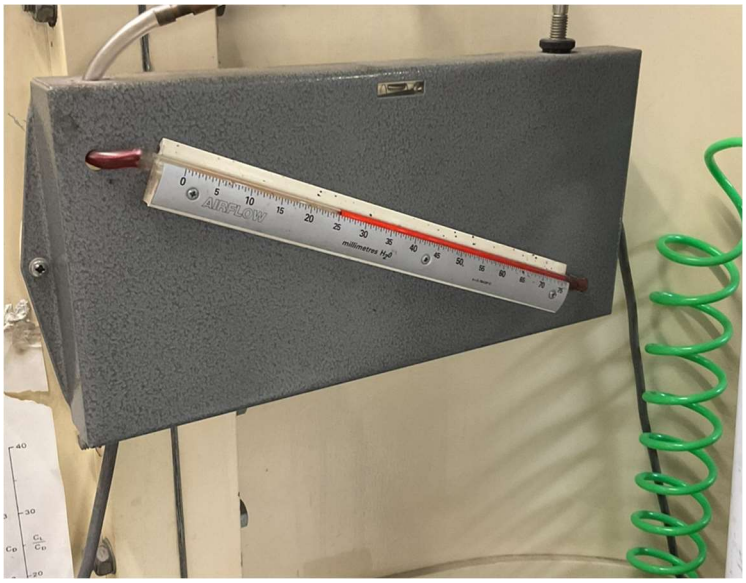

Fig 5. Water Manometer placed before test section measuring RPD in UCD Mechanical Lab

4.3 Techniques Used

Generating a desired Reynolds's number in wind tunnel:

1. To ensure that the flow through the wind tunnel is laminar – the flow through the wind tunnel is adjusted to a measure value on the manometer to get approximately 100,000 for the cylinder. A free stream velocity is obtained using the value from the manometer. The RPD value obtained from the differential pressure transducer is obtained. Wait 5 minutes for the flow to stabilize before noting the manometer reading.
2. Free stream total and static pressures are obtained also from the pitot static tube on the pressure display above the tunnel.
3. Once the model is mounted in the wind tunnel, the before and after values on the load cells AFT, BEF and DRAG must be noted for each model to calculate drag and lift accounting for the weight of the model.

Determining surface pressure of bluff body (cylinder):

1. When placing the model in the test section of the wind tunnel, ensure the pressure tap is facing upwards at 12 o'clock. This can be adjusted in the calculations afterwards. Beginning at -5 degrees angle of attack, adjust the angle of attack using the wheel mounted on the test section. Note the pressure on the differential manometer at each angle of attack from -5 degrees to 190 degrees at 5-degree intervals.

Determining drag and lift for NACA 0012:

1. Ensure the water manometer is at same value for the previous experiment to reach same Reynolds number.
2. Mount the airfoil in the test section. Ensure to note the load cell readings before and after mounting the model. Calculate the weight of the model.
3. From -5 degree to 18 degrees, change the angle of attack for the airfoil in increments of 1-degree while taking note of the load cell readings at each interval.

Notes:

Use of the water manometer to find the velocity and Reynolds number flow through the wind tunnel. The water manometer pressure reading for total pressure was used to calculate the free stream dynamic pressure in the wind tunnel instead of the pitot static tube due to convenience of the water manometer not depending on the density of the air inside the tunnel using the pitot static tube.

6. Experimental Results

5.1 Bluff Body: the smooth cylinder

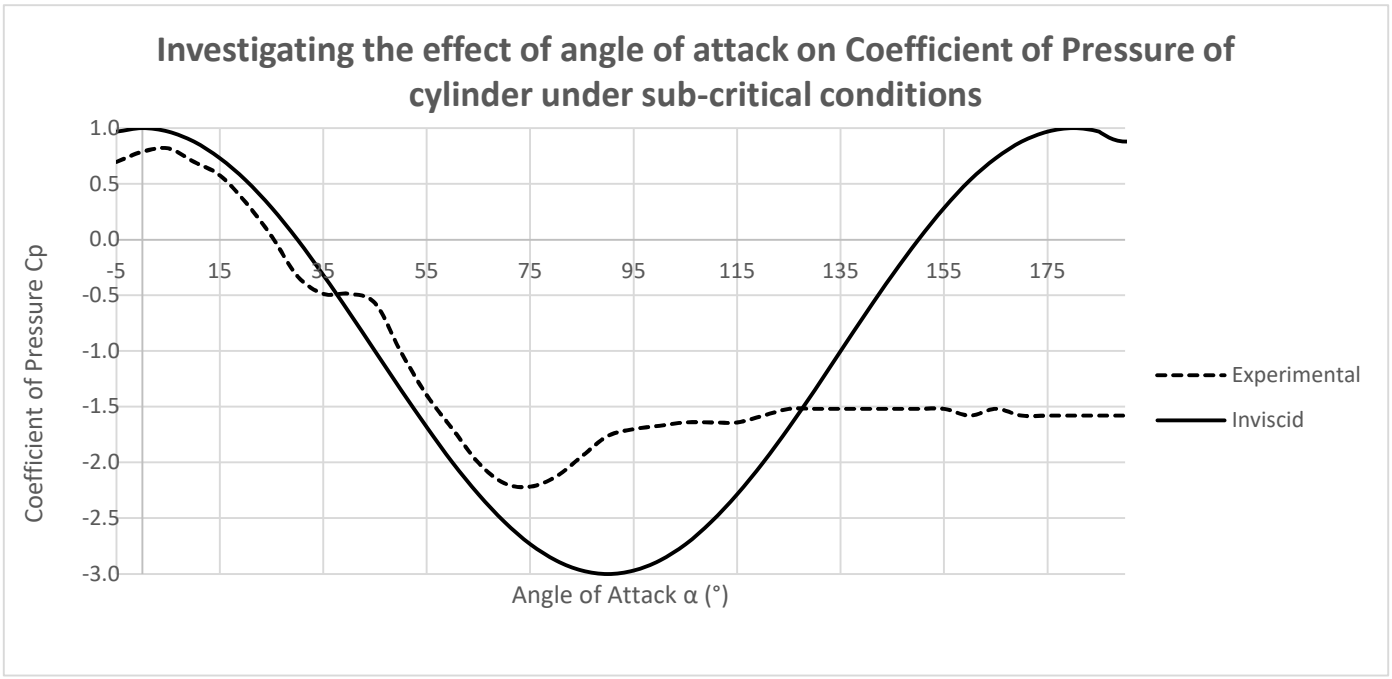

Graph 1. Coefficient of pressure against the angle of attack on flow over the cylinder

Table 1. Values obtained in the wind tunnel compared to the desired values for the bluff body (cylinder)

	Measurements	
	Desired	Obtained (RPD reading)
Reynolds Number	100,000	85183.6
Velocity (m/s)	19.68	16.77

5.2 Streamlined Body: NACA 0012 Airfoil

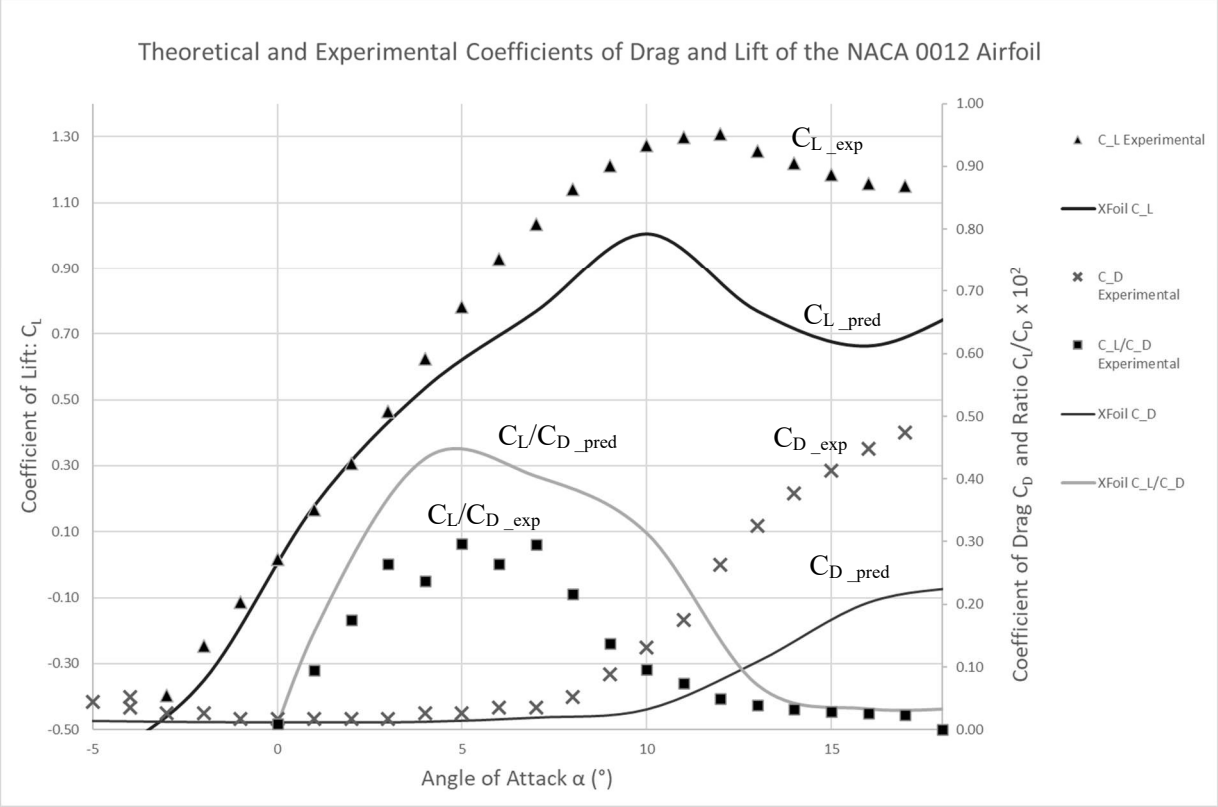

Graph 2. Coefficients of Lift and Drag against the angle of attack on a NACA 0012 airfoil. Plots of predicted values from Xfoil software for Reynold's number; 170,367, which was obtained experimentally, for comparison.

Table 2. Values obtained in the wind tunnel compared to the desired values for the streamlined body (NACA 0012 airfoil)

		Measurements
	Desired	Obtained (RPD reading)
Reynolds Number	200,000	170367
Velocity (m/s)	19.68	16.77

Table 3. Calculation of the weight of the NACA 0012 Airfoil

Load Cells: NACA 0012 Airfoil		
1	2	3
-5.2	-2.9	0
-0.01	0	0.01
-5.21	-2.9	0.01
Weight (N):		8.11

7. Discussion

Graph 1:

- The inviscid solution for flow over the cylinder is periodic and returns to a value of 1 at 180˚ versus the viscous experimental solution levels off after reaching a minimum C_P value of -2.2.
- The minimum C_P value is shown to be at a lower angle of attack than the inviscid solution which shows that the surface pressure tap was not at exactly 0˚ when beginning the experiment. This can be backed since the cylinder should have a C_P value of 1 at 0 ˚ due to zero velocity at the stagnation point. The cylinder shows a maximum value of 0.8 for C_P instead of 1.
- There shows to be only one stagnation point for the viscous solution since the curve does not return to a value of 1. This shows a separation point after a maximum velocity is obtained at an experimental angle of 75 ˚.
- Maximum velocity occurs at an earlier angle of attack for the viscous solution at 75 ˚ versus 90 ˚ for the inviscid solution.
- For the inviscid solution, the periodicity of the curve shows that the flow is attached to the body and there is no separation, like creeping flow. Whereas the experimental solution shows the separation at the minimum C_P reading at the point of separation of the boundary layer with the body. Wakes and turbulence are predicted downstream of the body due to this separation, as shown in Figure 4.
- By comparing inviscid to viscous solutions, one can note that the boundary layer relies on viscous forces to separate from the body that it is formed over.

Graph 2:

- Coefficient of Lift: For the NACA 0012, the stall angle is shown at maximum lift of 12˚ angle of attack. For the Xfoil theoretical solution, the stall angle is earlier at approximately 10 ˚. This can be attributed to the accuracy of setting the airfoil exactly horizontal for 0 ˚. For low angles of attack the coefficient of lift behaves linearly with α. In this region, the flow is attached and behaves smoothly.
- Coefficient of Drag: A higher coefficient of drag was found experimentally to be higher than the Xfoil theoretical curve. This can be due to the turbulence in the wind tunnel. Although the flow is considered completely laminar, and there is a sheet in place, to reduce turbulence, but this cannot be guaranteed.
- Ratio of Coefficient of Lift to Coefficient of Drag: The Xfoil theoretical solution shows to be higher than the experimental data found. Therefore, the experimental airfoil shows lower performance regarding drag and lift than the theoretical solution.
- Shown on Graph 2, the Coefficient of lift does not begin at 0 for 0 angle of attack as it should, which shows that the model was not completely horizontal for the set up in the test section. By beginning the experiment at -5-degree angle of attack, one can calculate the actual angle for a value of 0 C_L. This value was 0.867˚ for the data obtained.
- Due to the symmetry of the NACA 0012, there is no lift generated when there is 0 degrees for the angle of attack.
- For application the of airfoils, an ideal angle of attack for maximum lift with reduced drag is at the maximum coefficient of lift of 1.31.

Assumptions:

- Quasi-one-dimensional flow.
- No turbulence within the wind tunnel test section.
- No losses in the airflow due to the friction of the tunnel walls and drag on the aerodynamic model.
- Air is incompressible within the tunnel.

These are some of the assumptions made to analyse the experimental data. These assumptions can result in the difference in the theoretical and the experimental solutions obtained. For example, assuming no air escaping the tunnel and no friction from the walls of the tunnels can result in a pressure loss and decrease in the velocity of the air, affecting the lift and drag on the model tested.

Difference in Experimental Velocity/Reynold's Number:

Due to the assumptions mentioned above, the difference in Reynolds number, shown in Table 1. and 2. can be attributed to the losses within the wind tunnel. Human error can also be a factor when reading the water manometer for the total pressure reading. If the Reynolds number was below the desired condition, it was said to be laminar flow and the experiment was continued.

8. Conclusions

Inviscid flow has unseparated flow due to the absence of viscous forces, which reduces downstream turbulence and keeps the boundary layer attached to the body which it is flowing over. Actual, experimental, viscous flow has separated flow after the maximum velocity at the minimum coefficient of pressure C_P. It can be assumed that flow is turbulent downstream of the cylinder due to this separation. Viscous flow has only one stagnation point due to the separation of the boundary layer.

The force of lift on a streamlined body is higher than the force of drag on the body for smaller angles of attack. The performance of an airfoil can be analysed using coefficients of lift and drag. A higher C_L/C_D ratio results in higher performance due to the reduced drag which is an undesired force on airfoils.

The stall angle for the NACA 0012 is approximately 12˚ angle of attack. After a maximum lift is obtained, the drag increases due to the increase in pressure drag. This angle is very important in aerospace as the angle of stall for a plane affects stalling speed. It is noted that this value is slightly smaller than expected as there is expected turbulence in the wind tunnel which would result in the thicker boundary layer attaching for a higher angle of attack. This can be attributed to experimental error.

At low angles of attack α, the flow over the airfoil is smooth and attached with minimum friction drag. As α becomes larger the flow separates on the top surface of the airfoil resulting in a 'dead air' region. In this region there is reversed flow as the air recirculates against the free stream flow. This is due to viscosity. (Anderson, 2007)

The zero-lift angle of attack should be 0 ° but is 0.867 ° for this analysis of the NACA 0012 due to its symmetry. This is due to the initial positioning of the airfoil in the testing section.

Both C_L and C_D are affected by the Reynold's number which can be expected as drag and lift are both affected by viscous effects.

The effects on aerodynamic forces such as pressure, drag and lift can be due to many factors, these include:

- Geometry of body
- Angle of attack/pitching angle
- The model scale and size
- Compressibility of the fluid
- Free-stream velocity/ Reynold's number (viscosity)
- Mach number (compressibility)

9. Bibliography

Anderson, J. D. (2007) *Fundamentals of Aerodynamics.* McGraw-Hill Higher Education.

Bertin, J. J. and Cummings, R. M. (2009) *Aerodynamics for Engineers.* 5th Edition edn.: Pearson Education International.

Bilstein, R. E. (1989) *Orders of Magnitude: A History of the NACA and NASA.* National Aeronautics and Space Administrtion, Office of Management , Scientific and Tchninal Information Division.

Dyke, M. V. (1982) *An Album of Fluid Motion.* Department of Mechanical Engineering Stanford University, Stanford, California: The Parabolic Press.

Gerhart, P. M., Gerhart, A. L. and Hochstein, J. I. (2017) *Munson's Fluid Mechanics.* 8th edn.: Wiley.

Grosz, P. M., Haddow, G. and Schiemer, P. (1993) *Austro-Hungarian Army Aircraft of World War One.* Flying Machines Press.

Nastase, A. (2008) '8 - Computation of the Friction Drag Coefficients of the Flying Configurations', *Computation of Supersonic Flow over Flying Configurations*. Amsterdam: Elsevier, pp. 256-268.

O'Rourke, D. M. 2022. MEEN40020 Laboratory Handout. University College Dublin.

Rudmin, D., Benaissa, A. and Poirel, D. (2013) 'Detection of Laminar Flow Separation and Transition on a NACA-0012 Airfoil Using Surface Hot-Films', *Journal of Fluids Engineering,* 135, pp. 101104.

Sogukpinar, H. (2018) *The effects of NACA 0012 airfoil modification on aerodynamic performance improvement and obtaining high lift coefficient and post-stall airfoil.*

Straw, M. P. 'Computation and measurement of wind induced ventilation'.

Appendices

Appendix A: Calculations

Area S Calculation:

- Cylinder: Width*Diameter = Planform Area

0.076 x 0.455 = 0.163 m^2

- Airfoil: Chord Length* Width =Planform Area

0.152 x 0.355 = 0.06916 m^2

Dynamic Pressure for Velocity/Reynolds Number Calculation:

Velocity = $\sqrt{(2*P/\rho)}$ (m/s)

$P = \text{Total Pressure} - \text{Static Pressure}$ (Pa)

Finding point of actual 0 degrees for airfoil – Interpolation between points closest to 0 for C_L.

Value obtained: 0.867 ˚ offset required to obtain graph that begins at zero lift at angle of attack 0.

Appendix B: Experimental and Theoretical Data

Part 1: Cylinder

Table B1: Data obtained experimentally for the cylinder at a Reynolds number of 85183.6

Angle (°)	Pressure (Pa)	Cp
-5	195	0.7
0	210	0.8
5	215	0.8
10	195	0.7
15	175	0.6
20	135	0.3
25	85	0.0
30	26	-0.3
35	0	-0.5
40	0	-0.5
45	-14	-0.6
50	-86	-1.0
55	-150	-1.4
60	-200	-1.7
65	-250	-2.0
70	-280	-2.2
75	-285	-2.2
80	-270	-2.1
85	-240	-1.9
90	-210	-1.8
95	-200	-1.7
100	-195	-1.7
105	-190	-1.6
110	-190	-1.6
115	-190	-1.6
120	-180	-1.6
125	-170	-1.5
130	-170	-1.5
135	-170	-1.5
140	-170	-1.5
145	-170	-1.5
150	-170	-1.5
155	-170	-1.5
160	-180	-1.6
165	-170	-1.5
170	-180	-1.6
175	-180	-1.6
180	-180	-1.6
185	-180	-1.6
190	-180	-1.6
355	195	0.7

Table B2: Data obtained using Equation 5. For inviscid theoretical solution for cylinder.

Inviscid Solution	
Angle	Cp
-5	0.97
0	1.00
5	0.97
10	0.88
15	0.73
20	0.53
25	0.29
30	0.00
35	-0.32
40	-0.65
45	-1.00
50	-1.35
55	-1.68
60	-2.00
65	-2.29
70	-2.53
75	-2.73
80	-2.88
85	-2.97
90	-3.00
95	-2.97
100	-2.88
105	-2.73
110	-2.53
115	-2.29
120	-2.00
125	-1.68
130	-1.35
135	-1.00
140	-0.65
145	-0.32
150	0.00
155	0.29
160	0.53
165	0.73
170	0.88
175	0.97
180	1.00
185	0.97
190	0.88

Part 2: NACA 0012 Airfoil

Table B3: Data obtained from Xfoil Software at Reynolds number 170,367 with NACA 0012 airfoil

X foil Values			
Angle of attack (˚)	Cl	Cd	Cl/Cd x 100
-5	-0.6175	0.01374	-0.449418
-2	-0.3516	0.01186	-0.296459
1	0.1787	0.01147	0.155798
4	0.5351	0.01238	0.432229
7	0.7675	0.019	0.403947
10	1.005	0.03208	0.313279
13	0.76883	0.10827	0.07101
16	0.6628	0.20265	0.032707
19	0.7927	0.23114	0.034295

Table B4: Data obtained from Xfoil Software at Reynolds number 170,367 with NACA 0012 airfoil

Experimental Values			
Angle (˚)	C_D	C_L	C_L/C_D
-5.00	0.05	-0.86	-16.33
-4.00	0.04	-0.70	-16.00
-3.00	0.04	-0.57	-16.25
-2.00	0.03	-0.40	-15.00
-1.00	0.03	-0.25	-9.33
0.00	0.02	-0.11	-6.50
1.00	0.02	0.02	1.00
2.00	0.02	0.17	9.50
3.00	0.02	0.31	17.50
4.00	0.02	0.47	26.50
5.00	0.03	0.62	23.67
6.00	0.03	0.78	29.67
7.00	0.04	0.93	26.50
8.00	0.04	1.04	29.50
9.00	0.05	1.14	21.67
10.00	0.09	1.21	13.80
11.00	0.13	1.27	9.67
12.00	0.18	1.30	7.40
13.00	0.26	1.31	4.97
14.00	0.32	1.26	3.86
15.00	0.38	1.22	3.23
16.00	0.41	1.19	2.87
17.00	0.45	1.16	2.59
18.00	0.47	1.15	2.43